Published Ahead of Print on June 4, 2021 as 10.1212/WNL.0000000000012326

OPEN

Neurology®
The most widely read and highly cited peer-reviewed neurology journal
The Official Journal of the American Academy of Neurology

AMERICAN ACADEMY OF NEUROLOGY®

Neurology Publish Ahead of Print
DOI: 10.1212/WNL.0000000000012326

Chronic White Matter Inflammation and Serum Neurofilament Levels in Multiple Sclerosis

Pietro Maggi, MD, PhD,[1,2*] Jens Kuhle, MD, PhD,[3*] Sabine Schädelin, MSc,[4] Franziska van der Meer,[ψ] PhD,[5] Matthias Weigel, PhD,[3,6,7] Riccardo Galbusera, MD,[3,6], Amandine Mathias, PhD,[2] Po-Jui Lu, MSc,[3,6] Reza Rahmanzadeh, MD,[3,6] Pascal Benkert, PhD,[4] Francesco La Rosa, MSc,[8,9] Meritxell Bach Cuadra, PhD, [8,9] Pascal Sati, PhD,[10,11] Marie Théaudin, MD,[2] Caroline Pot, MD, PhD,[2] Vincent van Pesch, MD, PhD,[1] David Leppert, MD,[3] Christine Stadelmann, MD,[5] Ludwig Kappos, MD,[3] Renaud Du Pasquier, MD,[2] Daniel S. Reich, MD, PhD,[11,12] Martina Absinta, MD, PhD,[11,12**] Cristina Granziera, MD, PhD,[3,6**]

ψ deceased on Nov 9th, 2020.

[1]Department of Neurology, Cliniques universitaires Saint-Luc, Université catholique de Louvain, Brussels, Belgium

[2]Department of Neurology and [3]Department of Radiology, Lausanne University Hospital and Lausanne University, Lausanne Switzerland

[3]Neurologic Clinic and Policlinic, MS Center and Research Center for Clinical Neuroimmunology and neuroscience Basel (RC2NB), Departments of Medicine, Clinical Research and Biomedical Engineering, University Hospital Basel and University of Basel, Basel, Switzerland

[4]Clinical Trial Unit, Department of Clinical Research, University Hospital Basel and University of Basel, Basel, Switzerland

[5]Institute of Neuropathology, University Medical Center Göttingen, Göttingen, Germany

[6]Translational Imaging in Neurology (ThINk) Basel, Department of Biomedical Engineering, Neurology Clinic and Policlinic and RC2NB, University of Basel and University Hospital Basel, Basel, Switzerland

[7]Radiological Physics, Department of Radiology, University Hospital Basel, Basel, Switzerland

[8]Signal Processing Laboratory (LTS5), Ecole Polytechnique Fédérale de Lausanne, Lausanne, Switzerland

[9]CIBM Center for Biomedical Imaging (CIBM), Lausanne, Switzerland

[10]Department of Neurology, Cedars-Sinai Medical Center, Los Angeles, CA, USA

[11]Translational Neuroradiology Section, National Institute of Neurological Disorders and Stroke, National Institutes of Health, Bethesda, MD, USA

[12]Department of Neurology, Johns Hopkins University, Baltimore, MD, USA.

*P.M. and J.K. contributed equally; **M.A. and C.G. contributed equally

Manuscript body/abstract word count: 3830/258

Title character count (with spaces max allowed 140): 87

Number of figures/tables: 4/1

Supplementary figures/tables: 3/3 (https://doi.org/10.5061/dryad.pk0p2ngn3)

Number of references: 40

Contact information for the corresponding author:
Prof. C. Granziera
Email: Cristina.granziera@usb.ch.

Study Funding: This study was partially supported by the Intramural Research Program of NINDS, NIH, US. This study was partially supported by the European Union's Horizon 2020 research and innovation pro-gram under the Marie Sklodowska-Curie project TRABIT (agreement No 765148) and by the CIBM Center for Biomedical Imaging.

Disclosure: Jens Kuhles work is supported by the Swiss National Science Foundation (320030_189140/1). Cristina Granziera is supported by the Swiss National Science Foundation (SNSF) grant PP00P3_176984, the Stiftung zur Förderung der gastroenterologischen und all-gemeinen klinischen Forschung and the EUROSTAR E!113682 HORIZON2020. Martina Absinta is supported by the Conrad N. Hilton Foundation (grant #17313). The other authors report no funding or support directly relevant to the manuscript.

Running head: Paramagnetic rims and serum neurofilaments in MS
Search Terms: Multiple Sclerosis; MRI
Keywords: paramagnetic rims, serum neurofilaments, chronic inflammation

Abbreviations: MS, multiple sclerosis; PRL, paramagnetic rim lesions; sNfL, serum neurofilament light chain; Gd, gadolinium; MSSS, MS disease severity scale; EDSS, expanded disability status scale; DMT, disease-modifying treatment; RRMS, relapsing-remitting MS; PMS, primary or secondary progressive MS; EPI, echo-planar-imaging sequence; KiM1P, mouse anti-CD68-macrophage/activated microglia antibody; APP, mouse anti-β-amyloid-precursor-protein; MBP, rabbit anti-myelin-basic-protein. IQR, inter-quartile-range

Abstract

Objective

To assess whether chronic white matter inflammation in multiple sclerosis (MS) patients - as detected *in-vivo* by paramagnetic rim MRI lesions (PRL) - is associated with higher serum neurofilament light chain (sNfL) levels, a marker of neuro-axonal damage.

Methods

In 118 MS patients with no gadolinium-enhancing lesions or recent relapses, we analyzed 3D-submillimeter phase MRI and sNfL levels. Histopathological evaluation was performed in 25 MS lesions from 20 additional autopsy MS patients.

Results

In univariable analyses, participants with ≥2 PRL ("PRL ≥2", n=43) compared to those with ≤1 PRL ("PRL 0–1," n=75) had higher age-adjusted sNfL percentiles (median, 91 and 68; p<0.001) and higher MS disease severity scale (MSSS median, 4.3 and 2.4; p=0.003). In multivariable analyses, sNfL percentile levels were higher in PRL ≥2 cases (β_{add}: 16.3; 95% CI: 4.6–28.0; p<0.01), whereas disease-modifying treatment (DMT), EDSS, and T2 lesion load did not affect sNfL. In a similar model, sNfL percentile levels were highest in cases with ≥4 PRL (n=30; β_{add}: 30.4; 95% CI, 15.6–45.2; p<0.01). Subsequent multivariable analysis revealed that PRL ≥2 cases had also higher MSSS (β_{add}: 1.1; 95% CI, 0.3–1.9; p<0.01), whereas MSSS was not affected by DMT or T2 lesion load. On histopathology, both chronic active and smoldering lesions exhibited more severe acute axonal damage at the lesion edge than in the lesion center (edge vs center: p=0.004 and p=0.0002, respectively).

Interpretation

Chronic white matter inflammation was associated with increased levels of sNfL and disease severity in non-acute MS patients, suggesting that PRL contribute to clinically relevant, inflammation-driven neurodegeneration.

Introduction

An important unmet clinical and research need for multiple sclerosis (MS) patients is the understanding of the clinical and pathological impact of ongoing chronic inflammation within the central nervous system (CNS), which may become the target of future disease-modifying treatment (DMT).

MS is a chronic neuroinflammatory and neurodegenerative disease characterized by focal demyelinated lesions scattered throughout the CNS.[1] New active MS lesions are characterized by overt inflammation with blood-brain-barrier (BBB) damage and are visible on MRI as focal areas of gadolinium (Gd) enhancement. After the first phase of acute demyelination, a subset of these lesions retains chronic inflammation at the edge (termed "chronic active/smoldering lesions"). In the last decade, several MRI-histopathological validation studies[2–10] have shown that chronic active/smoldering lesions (although probably not all of them)[11] can be visualized on susceptibility-based MRI as non-Gd-enhancing lesions with a paramagnetic rim (PRL).[9,12–15]

The MRI susceptibility contrast at the lesion rim is mainly related to iron accumulation within activated microglia/macrophages,[2,3,7,16] though persistent oxidative stress may also contribute.[6,17–19] From a clinical point of view, PRL are frequent in both relapsing-remitting and progressive MS and are clinically associated with more aggressive disease.[8,14,20,21] Whether PRL are associated with increased neuroaxonal damage in living MS patients is currently unknown.

Neuropathology studies have shown that iron-rich activated microglia/macrophages and smoldering demyelination can be found at the edge of some chronic MS lesions,[7] which have been classified as "chronic active" or "smoldering" lesions depending on the amount of myelin phagocytosis observed.[22,23] Indeed, chronic inflammation and damage to myelin and axons fall on a spectrum making it sometimes difficult to accurately separate chronic active from smoldering lesions also in histopathological analyses. Axon loss and ongoing axon damage have been described, respectively, at the center and edge of such lesions,[6,10,24–26] and there is a correlation between axon injury and the number of chronic active and smoldering lesions in progressive MS cases.[20,25,27] Taken together, these results suggest that focal chronic inflammation can drive neurodegeneration.

Neuro-axonal damage is considered the substrate of permanent neurological disability,[28] and monitoring the levels of neurofilament proteins in the peripheral blood has shown promise as a marker of disease activity and neurodegeneration in MS.[29] Specifically, previous studies suggest that sNfL levels mirror not only diffuse neuronal loss but also focal inflammatory damage in MS: sNfL levels increase when acute Gd-enhancing lesions are present, correlating with the number of such lesions.[30] However, whether sNfL levels reflect the presence of chronic white matter inflammation — in the form of PRL — has not been investigated in vivo.

In this study, we assessed whether the presence of PRL in MS patients, as detected in vivo with susceptibility-based MRI, is associated with an increase in the levels of serum NfL. We also aimed to confirm and extend previous knowledge by showing that chronic active and smoldering lesions —the histopathological correlate of PRL — exhibit substantial axonal loss that colocalizes with chronic inflammatory cells and results in increased NfL release.

Methods

Assessment of the relationship between PRL and sNFL in vivo

Patients. For all participants, imaging, laboratory, and clinical data were collected between December 2017 and September 2019 in two university hospitals (University Hospital Basel and Lausanne University Hospital, Switzerland). Inclusion criteria were adults with a diagnosis of relapsing-remitting (RRMS), or primary or secondary progressive MS (PMS), according to the 2017 McDonald MS criteria,[31] and either untreated or on stable DMT for at least 3 months. Cases were excluded for subsequent analysis if they lacked matched imaging, laboratory, and clinical assessments within 6 months; had a clinical relapse or corticosteroid treatment within the 4 months preceding testing; had any Gd-enhancing lesions assessed in clinical MRI performed within 2 months of the study MRI; or had motion-corrupted MRI.

The imaging protocol included high-resolution, susceptibility-based MRI for PRL assessment (see below). Serum samples were collected, stored, and processed for sNfL analysis at the University Hospital Basel using the NF-Light® assay on single molecule array HDX platform (Quanterix, Billerica). Age-adjusted percentiles of sNfL were calculated in MS patients in

relationship to a database of 259 healthy controls (485 sNfL samples).[32] Clinical data included EDSS[33] and MSSS.[34] DMT were categorized as follows: (1) untreated; (2) injectable "platform" drugs with moderate efficacy, including glatiramer acetate and interferon beta-1a/b; (3) "oral" drugs with mostly high efficacy, including teriflunomide, dimethyl fumarate, and fingolimod; (4) "very-high-efficacy" drugs, including ocrelizumab, rituximab, natalizumab, and mitoxantrone.

Imaging acquisition and analysis. All participants underwent brain MRI on a 3T Magnetom Skyra or Prisma-fit scanner (Siemens Healthcare, Erlangen, Germany) in Lausanne (Switzerland) or a 3T Magnetom Prisma scanner (Siemens Healthcare, Erlangen, Germany) in Basel (Switzerland). Imaging at both centers included a high-resolution 3D segmented echo-planar-imaging (EPI) sequence providing T2*-weighted and phase contrasts (repetition time (TR), 64 ms; echo time (TE), 35 ms; flip angle (FA), 10°; echo-train length, 15; acquisition time (AT), 5 min 46 s; 288 sagittal slices; 0.65-mm isometric resolution) and a 3D T2-FLAIR sequence (TR, 5000 ms; TE, 391 ms; FA, variable; AT, 4 min 47 s; 176 sagittal slices; 1.0-mm isometric resolution). Additionally, 3D T1-weighted MPRAGE or MP2RAGE scans were acquired in Lausanne and Basel, respectively.

Phase postprocessing was performed as previously reported, with paramagnetic shifts rendered as hypointense.[6,18] For each participant, the presence of PRL on unwrapped phase images was independently assessed by 2 raters (PM and MA). In case of initial disagreement on the presence/absence of a specific PRL, agreement was reached in a separate session by consensus between the two raters. A chronic lesion was rated as a PRL when it showed a hypointense rim and internal isointensity to perilesional white matter on phase images.[8,12] Automated lesion segmentation was performed using FLAIR and MPRAGE/MP2RAGE images[35] and manually corrected if needed, yielding total white matter T2-hyperintense lesion volume ("T2 lesion load"). Brain volumes (gray matter volume + white matter volume/total intracranial volume) were computed using FreeSurfer (https://surfer.nmr.mgh.harvard.edu) after lesion filling on MPRAGE/MP2RAGE images.

Statistical analysis. Cases were initially categorized in 3 groups based on previous evidence from the literature according to the number of PRL (0, 1-3, ≥4);[8,15] due to the statistical distribution of the data in this particular study, we implemented a simpler cutoff of PRL 0–1 and ≥2. The interrater reliability for PRL groups was computed using Cohen's κ. Baseline differ-

ences (demographic and clinical) between PRL groups were assessed in a univariable analysis using t-test, Mann-Whitney U test, or chi-square test, as appropriate. The association between clinical and MRI measures and PRL (0–1 and ≥2; dependent variable) was assessed in a multivariable logistic model using MRI lesion load, disease duration, MS subtype, and DMT as covariates (estimates β_{OR} are back-transformed, indicating the odds ratio for ≥2 vs. 0–1 PRL). The number of PRL was assessed in a negative binomial model using the same independent variables (estimates β_{IRR} are back-transformed, indicating the PRL incidence rate ratio associated with unit increase in the respective covariate). To achieve an age-independent estimation of sNfL, levels were described as age-dependent percentiles derived from healthy controls, as previously described.[30]

The association between PRL categories and sNfL percentiles (dependent variable) was tested in a multivariable linear model using EDSS, MS subtype, MRI lesion load, and DMT as covariates (estimates β_{add} indicate the estimated increase in sNfL percentile). To compare our results to two recent studies,[8,15] we repeated the same analysis after grouping MS cases according to a different PRL number cutoff (0, 1–3, and ≥4). The association between PRL groups and MSSS (dependent variable) was assessed in a multivariable linear model using PRL number, MS subtype, MRI lesion load, and DMT as covariates (estimates β_{add} indicate the number of points MSSS is estimated to increase).

To exclude any possible influence of the different 3T scanners on the results, we repeated all analyses adding "scanner type" as covariate.

Standard Protocol Approvals, Registrations, and Patient Consents

For this study, we:

a. received approval from the local ethical standards committee on human experimentation.

b. received written informed consent was obtained from all patients participating in the study (consent for research).

The Consolidated Standards of Reporting Trials chart is provided in Supplementary Figure 1.

Assessment of the presence of acute axonal damage in histopathological correlates of PRL (chronic active/smoldering lesions):

Neuropathological analysis. Formalin-fixed, paraffin-embedded brain tissue was randomly selected from archival autopsy MS cases that had been collected at the Institute of Neuropathology at the University Medical Center Göttingen.

Neuropathological evaluation of lesions at different histopathological stages[22,23] was performed to assess the extent of acute axonal damage in relation to macrophage infiltration/microglia activation and ongoing demyelination in both the lesion core and edge. Paraffin-embedded 2–3-µm-thick tissue sections were deparaffinized, stained with HE (hematoxylin and eosin), LFB/PAS, (Luxol fast blue/periodic acid-Schiff, myelin), Bielschowsky's silver impregnation method (axons), and immunohistochemistry according to standard procedures. Primary antibodies were diluted in blocking buffer and incubated over night at 4°C. Antibody binding was visualized using biotinylated secondary antibodies (GE Healthcare, Jackson ImmunoResearch and DCS Innovative Diagnostic Systems), peroxidase-conjugated avidin and 3,3'-diminobenzidine (DAB; Sigma-Aldrich). Double-labelling immunohistochemistry was performed combining DAB and Fast Blue using alkaline phosphatase-conjugated secondary antibody (Dako). The following primary antibodies were used: mouse anti-CD68-macrophage/activated microglia antibody (clone KiM1P,1:50, kind gift of Prof. Dr. Heinz-Joachim Radzun, Göttingen), mouse anti-β-amyloid-precursor-protein (APP; Merck Millipore, MAB348, clone 22C11, 1:2000), and rabbit anti-myelin-basic-protein (MBP; Dako, A0623, 1:2000). Quantitative analysis of APP-positive (APP+) axonal spheroids (acutely injured axons), CD68-positive macrophages/activated microglia and MBP-containing phagocytes was performed using a 10x10 ocular morphometric grid (400x magnification; Olympus, Japan). The results were expressed as cells/mm^2.

MRI-pathology. One MS brain was imaged on a 3T Prisma MR system using a 20-channel head-and-neck coil and a dome-shaped brain-container filled with perfluoropolyether. The brain was fixed in 4% formalin within 24 hours from the time of death and for 4 months before the MRI. Postmortem unwrapped phase images were obtained from a 3D-EPI acquisition (330-µm isometric, TR=65ms, TE=35ms, ETL=13, bandwidth 394Hz/Pixel). The matching between MRI and histopathology was achieved through a personalized 3D-printed cutting box.[36] Additional manual registration between the digitized brain slab surfaces and the corresponding MRI slices was performed to further refine the match between histopathological and MRI images. Immunohistochemistry for myelin, microglia/macrophages and acute axon-

al injury was obtained using anti-myelin-basic-protein (MBP), MHC class II (clone CR3/43, hereafter "MHC II") and anti-β-amyloid-precursor-protein (APP; Chemicron) antibodies; ferrous iron (Fe^{2+}) was visualized using Turnbull staining as previously described.[3,22]

Statistical analysis. Differences in APP+ spheroid densities between the center and the edge of lesions available for neuropathological analysis were assessed using the Mann-Whitney U test. Differences in CD68+ phagocyte density and MBP+ phagocyte density between early active, chronic active, smoldering and chronic inactive lesions were assessed using one-way ANOVA and Kruskal-Wallis test with Dunn's multiple comparison test. To assess a possible correlation between APP+ spheroids and CD68+ activated microglia/macrophages at the lesion edge, nonparametric Spearman's correlation was used. Statistical analysis was performed using R version 3.6.3 (2020-02-29) and Prism version 6.0 (GraphPad).

Data availability

Anonymized data will be shared by reasonable request from the principal investigator.

Results

Assessment of the relationship between PRL and sNFL in vivo

Participant characteristics. Of 137 consecutively screened adults with MS, 118 (86%) were included in this study (10 were excluded because of motion artifacts and 9 because of the presence of Gd-enhancing lesions); 86 (73%) had RRMS and 32 (27%) had PMS.

Overall, 70/118 participants (59%) had ≥1 PRL, 43 (36%) had ≥2 PRL, and 30 (25%) had ≥4 PRL. Among PMS patients, 22/32 (69%) had ≥1 PRL, 18/32 (56%) had ≥2 PRL and 13/32 (41%) had ≥4 PRL; among RRMS patients, 48/86 (56%) had ≥1 PRL, 29/86 (34%) had ≥2 PRL and 17/86 (20%) had ≥4 PRL. Cohen's κ for the interrater reliability of PRL assessment was 0.83. The median time-lapse between MRI acquisition and clinical-laboratory assessment was 15 days (inter-quartile-range [IQR], 1.5–36, and range, 0–174). Only 14 of 118 patients (12%) had a blood sample performed more than 60 days from the MRI.

Based on our previous observations [8,15], cases were initially categorized in 3 groups according to the number of PRL (0, 1-3, and ≥4; Supplementary Table 1). However, due to the distribution of the cohort data in this study, we implemented a simpler cutoff of PRL 0–1 and ≥2. Thus, hereafter, cases without PRL or with only 1 PRL are termed "PRL 0–1" (n=75, 64%), whereas cases with ≥2 PRL are termed "PRL ≥2" (n=43, 35%). Figure 1 shows representative MRI images of PRL 0–1 and PRL ≥2 MS cases and their respective sNFL percentiles, and Table 1 lists clinical, laboratory, and MRI characteristics.

Of the 118 patients included in the study, 28 (24%) were untreated (14 RRMS and 14 PMS). The percentage of patients receiving DMT (including very-high-efficacy treatments) was similar between PRL 0–1 and PRL ≥2 cases. PRL ≥2 cases were more disabled (median EDSS score 3, IQR 3.5) than PRL 0–1 cases (median 2, IQR 2.5) (p=0.01), and this was true also when scaling EDSS by disease duration (median MSSS score, 4.3 [IQR 3.1] vs. 2.4 [IQR 3.16], respectively; p=0.003).[34]

T2-lesion load was higher in PRL ≥2 cases (p<0.001). Normalized brain volume (cortical plus white matter volumes/total intracranial volume) did not significantly differ between PRL 0–1 and PRL ≥2 cases. Similarly, we did not observe between-group differences for volumes of cortex, white matter, thalamus, or basal ganglia (putamen, pallidus and caudate) (Supplementary Figure 2). Finally, median sNfL percentile was higher in PRL ≥2 (median 91, IQR 20) than PRL 0–1 (median 68, IQR 43) cases (p<0.001). Segregation of cases according to both PRL status (PRL 0–1 and PRL ≥2) and different sNfL percentile thresholds (50^{th}, 80^{th}, and 90^{th}) is shown in the Supplementary Table 2.

Association between PRL and sNfL. PRL ≥2 cases had on average 16 percentile-point higher sNfL (β_{add}, 16.3; 95% CI, 4.6–28.0; p<0.01) compared to PRL 0–1 cases. No other covariate, including MS subtype (RRMS vs. PMS), DMT, EDSS, and T2-lesion load, showed an independent effect on sNfL levels (Figure 2A). Furthermore, cases with 1–3 PRL (n=40) and ≥4 PRL (n=30) had 15 and 30 percentile-point higher sNfL levels than cases with 0–1 PRL (β_{add}, 14.8; 95% CI, 3.2–26.3; p=0.01 and β_{add}, 30.4; 95% CI, 15.6–45.2; p<0.01, respectively). Again, no other covariate showed an effect on sNfL levels (Figure 2B).

Moreover, there was no association between normalized brain volume and sNfL in the model that included ≥ 2 PRL as independent variable. Also, there was no evidence that the differ-

ence in scanners influenced the association between brain volume and NfL percentiles (Supplementary Table 3).

Association between PRL and clinical-MRI measures. Higher T2-lesion load (per mL unit) and shorter disease duration (per year unit) were respectively associated with 21% and 7% higher odds of having PRL ≥2 (β_{OR}, 1.21; 95% CI, 1.12–1.33; p<0.01 and β_{OR}, 1.07; 95% CI, 1.01–1.14; p=0.02, respectively).

MS subtype (RRMS vs. PMS; β_{OR}, 0.99; 95% CI, 0.27–3.74; p=0.99) and current DMT, including oral (vs. platform, β_{OR}, 0.78; 95% CI, 0.21–3.05; p=0.72) and very-high-efficacy (vs. platform, β_{OR}, 0.93; 95% CI, 0.28–3.16; p=0.91), were not associated PRL ≥2 status.

Results were similar when using the number of PRL per case as the dependent variable: only higher T2-lesion load (β_{IRR}, 1.13 /mL; 95% CI, 1.09–1.18; p<0.01) and shorter disease duration (β_{IRR}, 1.05 /year; 95% CI, 1.01–1.08; p<0.01) were associated with the number of PRL.

Association between PRL and disease severity. Not surprisingly, MSSS was higher by 2.7 points in PMS vs. RRMS cases (β_{add}, 2.7; 95% CI, 1.4–3.6; p<0.01). In PRL ≥2 cases, MSSS was on average 1.1 points higher than in PRL 0–1 cases (β_{add}, 1.1; 95% CI, 0.3–1.9; p<0.01). No other covariate, including current DMT (oral: β_{add}, -0.8; 95% CI, -1.8–0.3; p=0.14; very-high efficacy: β_{add}, 0.1; 95% CI, -0.7–1.0; p=0.75), and T2-lesion load (β_{add}, -0.02; 95% CI, -0.07–0.04; p=0.54), was associated with MS severity.

Assessment of the presence of acute axonal damage in histopathological correlates of PRL (chronic active/smoldering lesions)

From an additional group of 20 autopsy MS patients (19 PMS/1 RRMS, 8 women/12 men, mean age 52 years, range 28–67), we studied the following MS lesions classified according to their pathological stage:[22,23] early active (n=4), chronic active (n=6), smoldering (n=9), and chronic inactive (n=6). Quantification of CD68+ activated microglia/macrophages and CD68+ phagocytes containing MBP+ particles (Supplementary Figure 3) showed that chronic active and smoldering lesions fall on a spectrum of inflammatory demyelinating activity at the lesion edge and an hypocellular core.[22,23].

Acutely injured axons (APP+) were rarely observed both in the center or at the edge of chronic inactive lesions. On the other hand, in chronic active/smoldering lesions, APP+ injured axons colocalized with the active edge of CD68+ macrophages/activated microglia, some of which contained MBP (Figure 3A). Quantitative analysis of acutely injured axons showed: (1) in chronic active/smoldering lesions (Figure 3B,C), the median number of APP+ spheroids per mm^2 was higher at the lesion edge (149.3 [IQR 104.9] and 52.3 [IQR 129.6]) than at the lesion center (19.6 [IQR 52.0] and 6.4 [IQR 8.3]; p=0.004 and p=0.0002); and (2) in chronic inactive lesions (Figure 3D), APP+ spheroids were only rarely found both at the lesion edge and in the lesion center (median 3.3 [IQR 16.4] and 3.8 [IQR 32.8]; p=0.46). The density of APP+ axonal spheroids positively correlated with the density of CD68 macrophages/activated microglia at the edge of chronic active/smoldering and chronic inactive lesions (r=0.86; p<0.0001; Figure 3E).

Finally, we acquired postmortem 3D-EPI images in a 59-year-old man with PMS (disease duration 24 years, EDSS=8 prior to death) and performed a matched MRI-histopathological assessment of one exemplary chronic active lesion. This chronic active lesion, which featured a paramagnetic rim on 3D-EPI phase MRI, showed ongoing inflammatory demyelination with iron accumulation as well as acute axonal damage at the lesion edge (Figure 4).

Discussion

Our multicenter study provides clear evidence of a relationship between the presence of ≥2 PRL and higher levels of sNfL in MS patients (both RRMS and PMS) without acute disease activity, showing that PRL are associated with neuro-axonal degeneration that can be detected in vivo. Furthermore, our postmortem evaluation shows that the histological correlates of PRL — chronic active and smoldering lesions — exhibit pronounced axon damage at the lesion edge, which colocalizes with chronic inflammatory cells.

In our in vivo study, the association between PRL and sNfL was independent of other factors previously shown to influence sNfL, such as age, T2-lesion load, and DMT (including very-high-efficacy DMT).[30,37,38] This somewhat surprising result may be partially explained by the fact that we studied a cohort with neither clinical nor radiological inflammatory activity,

whereas many other studies included both active and non-active patients. In addition, it is possible that the effects of those clinical factors may partially be mediated through PRL.

Importantly, our data show that most patients with PRL ≥2 (72%) had sNfL levels above the 80th percentile, a frankly pathological threshold according to previous studies.[30] Thus, our findings are relevant not only at the group level but also at the patient level (Supplementary Table 2). Discrepancies between sNfL levels and the presence/absence of PRL, observed in a minority of patients, require further investigation in larger cohorts and suggest that other factors may also play a role.

Surprisingly, the increase in sNfL that we described typically corresponds to only a handful of additional PRL in each case, indicating that even the limited amount of ongoing axon damage at the edge of chronic active/smoldering lesions - substantially less than what occurs in active lesion - can be detected in the serum. This profound focal damage also results in MRI-detectable expansion of some PRL over a period of a few years, such that these lesions are both larger and more T1-hypointense on MRI than other MS lesions.[6–8,10,24–26]

In our cohort of non-active MS patients, there was no difference in brain volume between PRL ≥2 and PRL 0–1 cases. This suggests that cross-sectional brain volume measurements — unlike PRL detection — do not provide a reliable snapshot of ongoing neuro-axonal destruction at the time of MRI.[39] Furthermore, despite the presence of a higher T2-lesion load in PRL ≥2 compared to PRL 0–1 patients, the number and volume of T2 lesions were not significantly related to sNfL levels, signifying that it is fundamental to identify the subtype of lesions that drives relentless neuro-axonal degeneration outside clinical and radiological relapses.

In agreement with recent evidence,[8,9,15] we found that PRL are frequent in both RRMS and PMS, with more than one-third of the patients (36%) harboring at least two PRL. We also found an inverse association between PRL and disease duration, supporting the idea that smoldering inflammation/demyelination at early disease stages might trigger clinical progression, but also that it might partially decline at the later stages of the disease. In addition, these data suggest that clinical estimates of disease duration are not reliable, especially in patients with insidious and progressive disease course.

Our work also extends previous findings[8,15,40] by showing that the reported association between PRL and clinical disability also holds in the absence of clinical or radiological signs of acute inflammation. Indeed, in our cohort, the association between PRL and MSSS was stronger than, and independent from, factors known to influence clinical outcomes in MS, such as T2-lesion load and very-high-efficacy DMT.

The histopathological analysis performed in this work provides additional evidence that the histopathological correlates of PRL — chronic active and smoldering lesions — exhibit high numbers of acutely injured axons (APP+ spheroids) at the lesion edge and lesion core, which lead to the release of axonal cytoskeleton proteins (including NfL) in CSF and blood. Here, acute axon injury and degeneration, leading to the release of neurofilaments (axonal cytoskeleton proteins) in the CSF and blood, was assessed using APP immunostaining, since APP transiently accumulates in acutely transected axon end-bulbs,[25,27,41] whereas neurofilament immunostaining reflects only past axon depletion.[42] In line with previous reports,[6,24–26,43] we showed that acute axonal injury and transection occur along with the inflammatory activity of activated macrophages and microglia in both chronic active and smoldering lesions, despite variable ongoing demyelination..

This study has some limitations. First, although serum samples were collected as close as possible to the MRI scan, in some cases (14/118, 12%) this time frame exceeded several months. While we cannot exclude that the "chronic inflammatory status" of such patients may have changed during this time gap, this is not likely considering the temporal persistence of PRL, which have been shown to last for at least several years.[7,10] Second, larger cohorts of participants are required to achieve adequate statistical power to consider the actual number of PRL per case (rather than dichotomizing or trichotomizing that number) in a multivariable analysis. Also, studies focusing on specific patients subgroups (eg. on early- vs late-stage RRMS patients) will have to be performed in the future. Regarding the effect of treatment, future longitudinal studies are required to investigate the differential effect (if any) of available DMT on these biomarkers.

In conclusion, we provide in vivo MRI and laboratory evidence that chronically inflamed lesions on MRI (PRL) are associated with elevated sNfL in people living with MS. The association between PRL and sNfL was strong and independent from other factors known to influence sNfL levels. Hence, we postulate that PRL may be a substantial driver of neuro-

axonal damage and clinical disability in patients without clinical or radiological signs of acute inflammation. This is a concept of key importance and further supports the role of PRL as a biomarker for patient stratification and treatment outcome in future clinical trials.

Acknowledgments

The authors thank the study participants; the neuroimmunology clinics at each center for recruiting and evaluating the patients and for coordinating the scans; Tobias Kober (Advanced Clinical Imaging Technology, Siemens Healthineers, Lausanne) and Jean-Baptiste Ledoux (TRM coordinator, service de "radiodiagnostic et radiologie interventionnelle," Lausanne University Hospital) for assistance with 3T MRI scan acquisition; the medical physics department at Basel University Hospital (USB) for hosting the study; and M.Sc. Marguerite Limberg for helping with patients enrollment at USB.

Funding

This study was partially supported by the Intramural Research Program of NINDS, NIH, US. Jens Kuhle's work is supported by the Swiss National Science Foundation (320030_189140/1). Cristina Granziera is supported by the Swiss National Science Foundation (SNSF) grant PP00P3_176984, the Stiftung zur Förderung der gastroenterologischen und allgemeinen klinischen Forschung and the EUROSTAR E!113682 HORIZON2020. Martina Absinta is supported by the Conrad N. Hilton Foundation (grant #17313). This study was partially supported by the European Union's Horizon 2020 research and innovation program under the Marie Sklodowska-Curie project TRABIT (agreement No 765148) and by the CIBM Center for Biomedical Imaging. The other authors report no funding or support directly relevant to the manuscript.

Competing Interests

Nothing to report.

Appendix 1. Authors

Name	Location	Contribution
Pietro Maggi, MD PhD	Université Catholique de Louvain	Design and conceptualized study; analyzed the data; drafted the manuscript for intellectual content
Jens Kuhle, MD PhD	University of Basel	Design and conceptualized study; analyzed the data; drafted the manuscript for intellectual content
Sabine Schaedelin, MSc	University of Basel	Analyzed, Interpreted the data; revised the manuscript for intellectual content
Franziska van der Meer, PhD	University of Göttingen	Analyzed, Interpreted the data; revised the manuscript for intellectual content
Matthias Weigel, PhD	University of Basel	Major role in the acquisition of data; revised the manuscript for intellectual content
Riccardo Galbusera, MD	University of Basel	Analyzed data, Interpreted the data; revised the manuscript for intellectual content
Amandine Matthias, PhD	University of Lausanne	Interpreted the data; revised the manuscript for intellectual content
Po-Jui Lu, MSc	University of Basel	Major role in the acquisition of data; revised the manuscript for intellectual content
Reza Rahmanzadeh, MD	University of Basel	Major role in the acquisition of data; revised the manuscript for intellectual content
Pascal Benkert, PhD	University of Basel	Analyzed, Interpreted the data; revised the manuscript for intellectual content
Francesco La Rosa, MSc	University of Lausanne	Analyzed, Interpreted the data; revised the manuscript for intellectual content
Merixtell Bach Cuadra, PhD	University of Lausanne	Interpreted the data; revised the manuscript for intellectual content
Pascal Sati, PhD	University of Lausanne	Interpreted the data; revised the manuscript for intellectual content

Marie Théaudin, MD	University of Lausanne	Interpreted the data; revised the manuscript for intellectual content
Carolin Pot, MD	University of Lausanne	Interpreted the data; revised the manuscript for intellectual content
Vincent Van Pesch, MD	Université Catholique de Louvain	Interpreted the data; revised the manuscript for intellectual content
David Leppert, MD	University of Basel	Interpreted the data; revised the manuscript for intellectual content
Christine Stadelmann, MD	University of Göttingen	Analyzed, Interpreted the data; revised the manuscript for intellectual content
Ludwig Kappos, MD	University of Basel	Interpreted the data; revised the manuscript for intellectual content
Renaud Du Pasquier, MD	University of Lausanne	Interpreted the data; revised the manuscript for intellectual content
Daniel S. Reich, MD PhD	National Institutes of Health	Conceptualized study; Interpreted the data; revised the manuscript for intellectual content
Martina Absinta, MD PhD	National Institutes of Health/ Johns Hopkins University	Design and conceptualized study; analyzed the data; drafted the manuscript for intellectual content
Cristina Granziera, MD PhD	University of Basel	Design and conceptualized study; analyzed the data; drafted the manuscript for intellectual content

References

1. Reich DS, Lucchinetti CF, Calabresi PA. Multiple Sclerosis. Longo DL, editor. New England Journal of Medicine. 2018 Jan 11;378(2):169–80.

2. Pitt D, Boster A, Pei W, Wohleb E, Jasne A, Zachariah CR, et al. Imaging Cortical Lesions in Multiple Sclerosis With Ultra–High-Field Magnetic Resonance Imaging. Archives of Neurology [Internet]. 2010 Jul 1 [cited 2020 Jun 22];67(7). Available from: http://archneur.jamanetwork.com/article.aspx?doi=10.1001/archneurol.2010.148

3. Bagnato F, Hametner S, Yao B, van Gelderen P, Merkle H, Cantor FK, et al. Tracking iron in multiple sclerosis: a combined imaging and histopathological study at 7 Tesla. Brain. 2011 Dec 1;134(12):3602–15.

4. Yao B, Bagnato F, Matsuura E, Merkle H, van Gelderen P, Cantor FK, et al. Chronic Multiple Sclerosis Lesions: Characterization with High-Field-Strength MR Imaging. Radiology. 2012 Jan;262(1):206–15.

5. Walsh AJ, Lebel RM, Eissa A, Blevins G, Catz I, Lu J-Q, et al. Multiple Sclerosis: Validation of MR Imaging for Quantification and Detection of Iron. Radiology. 2013 May;267(2):531–42.

6. Absinta M, Sati P, Schindler M, Leibovitch EC, Ohayon J, Wu T, et al. Persistent 7-tesla phase rim predicts poor outcome in new multiple sclerosis patient lesions. The Journal of clinical investigation. 2016 Jul 1;126(7):2597–609.

7. Dal-Bianco A, Grabner G, Kronnerwetter C, Weber M, Hoftberger R, Berger T, et al. Slow expansion of multiple sclerosis iron rim lesions: pathology and 7 T magnetic resonance imaging. Acta Neuropathologica. 2017 Jan;133(1):25–42.

8. Absinta M, Sati P, Masuzzo F, Nair G, Sethi V, Kolb H, et al. Association of Chronic Active Multiple Sclerosis Lesions With Disability In Vivo. JAMA Neurology [Internet]. 2019 Aug 12 [cited 2019 Aug 16]; Available from: https://jamanetwork.com/journals/jamaneurology/fullarticle/2747565

9. Kaunzner UW, Kang Y, Zhang S, Morris E, Yao Y, Pandya S, et al. Quantitative susceptibility mapping identifies inflammation in a subset of chronic multiple sclerosis lesions. Brain. 2019 Jan 1;142(1):133–45.

10. Dal-Bianco A, Grabner G, Kronnerwetter C, Weber M, Kornek B, Kasprian G, et al. Long-term evolution of multiple sclerosis iron rim lesions in 7 T MRI. Brain. 2021 Jan 23;awaa436.

11. Popescu BF, Frischer JM, Webb SM, Tham M, Adiele RC, Robinson CA, et al. Pathogenic implications of distinct patterns of iron and zinc in chronic MS lesions. Acta Neuropathol. 2017 Jul;134(1):45–64.

12. Absinta M, Sati P, Fechner A, Schindler MK, Nair G, Reich DS. Identification of Chronic Active Multiple Sclerosis Lesions on 3T MRI. American Journal of Neuroradiology. 2018 Jul;39(7):1233–8.

13. Clarke MA, Pareto D, Pessini-Ferreira L, Arrambide G, Alberich M, Crescenzo F, et al. Value of 3T Susceptibility-Weighted Imaging in the Diagnosis of Multiple Sclerosis. American Journal of Neuroradiology [Internet]. 2020 May 21 [cited 2020 Jun 1]; Available from: http://www.ajnr.org/lookup/doi/10.3174/ajnr.A6547

14. Blindenbacher N, Brunner E, Asseyer S, Scheel M, Siebert N, Rasche L, et al. Evaluation of the 'ring sign' and the 'core sign' as a magnetic resonance imaging marker of disease activity and progression in clinically isolated syndrome and early multiple sclerosis. Multiple Sclerosis Journal - Experimental, Translational and Clinical. 2020 Jan;6(1):205521732091548.

15. Maggi P, Sati P, Nair G, Cortese ICM, Jacobson S, Smith BR, et al. Paramagnetic Rim Lesions are Specific to Multiple Sclerosis: An International Multicenter 3T MRI Study. Annals of Neurology. 2020 Nov;88(5):1034–42.

16. Wisnieff C, Ramanan S, Olesik J, Gauthier S, Wang Y, Pitt D. Quantitative susceptibility mapping (QSM) of white matter multiple sclerosis lesions: Interpreting positive susceptibility and the presence of iron: Iron and Myelin Content of MS Lesions with MRI. Magnetic Resonance in Medicine. 2015 Aug;74(2):564–70.

17. Langkammer C, Liu T, Khalil M, Enzinger C, Jehna M, Fuchs S, et al. Quantitative Susceptibility Mapping in Multiple Sclerosis. Radiology. 2013 May;267(2):551–9.

18. Absinta M, Sati P, Gaitan MI, Maggi P, Cortese IC, Filippi M, et al. Seven-tesla phase imaging of acute multiple sclerosis lesions: a new window into the inflammatory process. Annals of neurology. 2013 Nov;74(5):669–78.

19. Gillen KM, Mubarak M, Nguyen TD, Pitt D. Significance and In Vivo Detection of Iron-Laden Microglia in White Matter Multiple Sclerosis Lesions. Frontiers in Immunology [Internet]. 2018 Feb 19 [cited 2020 Jun 22];9. Available from: http://journal.frontiersin.org/article/10.3389/fimmu.2018.00255/full

20. Frischer JM, Weigand SD, Guo Y, Kale N, Parisi JE, Pirko I, et al. Clinical and pathological insights into the dynamic nature of the white matter multiple sclerosis plaque: Dynamic Nature of MS Plaque. Annals of Neurology. 2015 Nov;78(5):710–21.

21. Luchetti S, Fransen NL, van Eden CG, Ramaglia V, Mason M, Huitinga I. Progressive multiple sclerosis patients show substantial lesion activity that correlates with clinical disease severity and sex: a retrospective autopsy cohort analysis. Acta Neuropathologica. 2018 Apr;135(4):511–28.

22. Kuhlmann T, Ludwin S, Prat A, Antel J, Brück W, Lassmann H. An updated histological classification system for multiple sclerosis lesions. Acta Neuropathologica. 2017 Jan;133(1):13–24.

23. Popescu BFGh, Lucchinetti CF. Pathology of Demyelinating Diseases. Annual Review of Pathology: Mechanisms of Disease. 2012 Feb 28;7(1):185–217.

24. Ferguson B. Axonal damage in acute multiple sclerosis lesions. Brain. 1997 Mar 1;120(3):393–9.

25. Singh S, Dallenga T, Winkler A, Roemer S, Maruschak B, Siebert H, et al. Relationship of acute axonal damage, Wallerian degeneration, and clinical disability in multiple sclerosis. Journal of Neuroinflammation [Internet]. 2017 Dec [cited 2020 Jun 21];14(1). Available from: http://jneuroinflammation.biomedcentral.com/articles/10.1186/s12974-017-0831-8

26. Prineas JW, Kwon EE, Cho ES, Sharer LR, Barnett MH, Oleszak EL, et al. Immunopathology of secondary-progressive multiple sclerosis. Annals of neurology. 2001 Nov;50(5):646–57.

27. Frischer JM, Bramow S, Dal-Bianco A, Lucchinetti CF, Rauschka H, Schmidbauer M, et al. The relation between inflammation and neurodegeneration in multiple sclerosis brains. Brain : a journal of neurology. 2009 May;132(Pt 5):1175–89.

28. Khalil M, Teunissen CE, Otto M, Piehl F, Sormani MP, Gattringer T, et al. Neurofilaments as biomarkers in neurological disorders. Nature reviews Neurology. 2018 Oct;14(10):577–89.

29. Cantó E, Barro C, Zhao C, Caillier SJ, Michalak Z, Bove R, et al. Association Between Serum Neurofilament Light Chain Levels and Long-term Disease Course Among Patients With Multiple Sclerosis Followed up for 12 Years. JAMA Neurology [Internet]. 2019 Aug 12 [cited 2019 Sep 5]; Available from: https://jamanetwork.com/journals/jamaneurology/fullarticle/2747563

30. Disanto G, Barro C, Benkert P, Naegelin Y, Schädelin S, Giardiello A, et al. Serum Neurofilament light: A biomarker of neuronal damage in multiple sclerosis: Serum NfL as a Biomarker in MS. Annals of Neurology. 2017 Jun;81(6):857–70.

31. Thompson AJ, Banwell BL, Barkhof F, Carroll WM, Coetzee T, Comi G, et al. Diagnosis of multiple sclerosis: 2017 revisions of the McDonald criteria. Lancet neurology. 2018 Feb;17(2):162–73.

32. Sutter R, Hert L, De Marchis GM, Twerenbold R, Kappos L, Naegelin Y, et al. Serum Neurofilament Light Chain Levels in the Intensive Care Unit: Comparison between Severely Ill Patients with and without Coronavirus Disease 2019. Ann Neurol. 2021 Mar;89(3):610–6.

33. Kurtzke JF. Rating neurologic impairment in multiple sclerosis: An expanded disability status scale (EDSS). Neurology. 1983 Nov 1;33(11):1444–1444.

34. Roxburgh RHSR, Seaman SR, Masterman T, Hensiek AE, Sawcer SJ, Vukusic S, et al. Multiple Sclerosis Severity Score: Using disability and disease duration to rate disease severity. Neurology. 2005 Apr 12;64(7):1144–51.

35. La Rosa F, Abdulkadir A, Fartaria MJ, Rahmanzadeh R, Lu P-J, Galbusera R, et al. Multiple sclerosis cortical and WM lesion segmentation at 3T MRI: a deep learning method based on FLAIR and MP2RAGE. NeuroImage: Clinical. 2020 Jun;102335.

36. Absinta M, Nair G, Filippi M, Ray-Chaudhury A, Reyes-Mantilla MI, Pardo CA, et al. Postmortem magnetic resonance imaging to guide the pathologic cut: individualized, 3-dimensionally printed cutting boxes for fixed brains. Journal of neuropathology and experimental neurology. 2014 Aug;73(8):780–8.

37. Kuhle J, Barro C, Disanto G, Mathias A, Soneson C, Bonnier G, et al. Serum neurofilament light chain in early relapsing remitting MS is increased and correlates with CSF levels and with MRI measures of disease severity. Mult Scler. 2016 Oct;22(12):1550–9.

38. Barro C, Benkert P, Disanto G, Tsagkas C, Amann M, Naegelin Y, et al. Serum neurofilament as a predictor of disease worsening and brain and spinal cord atrophy in multiple sclerosis. Brain. 2018 Aug 1;141(8):2382–91.

39. Bagnato F, Gauthier SA, Laule C, Moore GRW, Bove R, Cai Z, et al. Imaging Mechanisms of Disease Progression in Multiple Sclerosis: Beyond Brain Atrophy. Journal of Neuroimaging. 2020 May;30(3):251–66.

40. Elliott C, Belachew S, Wolinsky JS, Hauser SL, Kappos L, Barkhof F, et al. Chronic white matter lesion activity predicts clinical progression in primary progressive multiple sclerosis. Brain. 2019 Sep 1;142(9):2787–99.

41. Kornek B, Storch MK, Weissert R, Wallstroem E, Stefferl A, Olsson T, et al. Multiple Sclerosis and Chronic Autoimmune Encephalomyelitis. The American Journal of Pathology. 2000 Jul;157(1):267–76.

42. Kuhlmann T. Acute axonal damage in multiple sclerosis is most extensive in early disease stages and decreases over time. Brain. 2002 Oct 1;125(10):2202–12.

43. Trapp BD, Peterson J, Ransohoff RM, Rudick R, Mork S, Bo L. Axonal transection in the lesions of multiple sclerosis. The New England journal of medicine. 1998 Jan 29;338(5):278–85.

Table 1. Clinical, laboratory, and MRI demographics

	PRL 0–1 cases	PRL ≥2 cases	p-value
# patients	75	43	
MS subtype, n (%)			0.43
RRMS	57 (76%)	29 (67%)	
PPMS/SPMS	18 (24%)	14 (33%)	
Median age, years	45 (36–53)	45 (32–54)	0.75
Clinical data			
Treatment, n (%)			0.34
Untreated/platform	19 (25%)	12 (28%)	
Oral	27 (36%)	10 (23%)	
Very-high-efficacy	29 (39%)	21 (49%)	
Median disease duration, years	9 (5–19)	11 (5–15)	0.90
Median EDSS score	2.0 (1.5–4.0)	3.0 (2.0–5.5)	0.01
Median MSSS score	2.4 (1.5–4.6)	4.3 (3.1–6.2)	0.003
MRI data			
Median normalized brain volume	0.62 (0.58–0.74)	0.61 (0.56–0.77)	0.53
Median T2-lesion load, mL	2.2 (0.6–6.4)	7.8 (4.0–17.9)	<0.001
Laboratory data			
Median sNfL percentile	68 (41–84)	91 (77–97)	<0.001

Abbreviations: PRL, paramagnetic rim lesions; EDSS, expanded disability status scale; MSSS, multiple sclerosis severity score; Normalized brain volume, gray matter volume + white matter volume/total intracranial volume; sNfL, serum neurofilament light chain. Ranges are the 25^{th}–75^{th} percentiles.

Figure 1. Representative MRI images of PRL 0–1 and PRL ≥2 MS cases and respective sNfL percentiles. Axial 3-tesla T2*-weighted magnitude and phase MRI images of **(A)** a patient with PRL ≥2 (RRMS, 40 years old, male; number of PRL: 12) with high sNfL (98th percentile), and of **(B)** a patient with PRL 0–1 (SPMS, 64 years old, male; number of PRL: 0) with low sNfL (3rd percentile). PRL are visible in A (arrowheads) but not B (arrows). Insets show magnified views. **(C)** Age-adjusted sNfL percentiles for PRL 0-1 and PRL ≥2 patients (A-B, crosses) and for the 118 MS patients included in the study (dots). Colored lines represent the percentile levels.

Abbreviations: RRMS, relapsing-remitting MS; PMS, primary/secondary progressive MS; PRL, paramagnetic rim lesions; sNfL: serum neurofilament light chain.

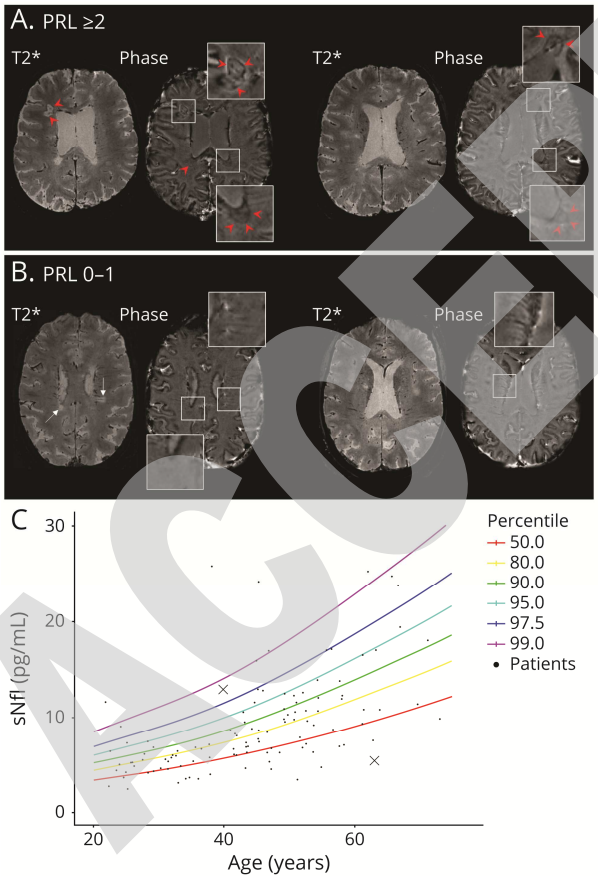

Figure 2. Paramagnetic rim lesions strongly and uniquely predict serum neurofilament light levels. (A) Estimated effects of T2-lesion load, MS subtype, EDSS, oral and very-high-efficacy DMT, and the presence of ≥2 PRL, as compared to 0–1 PRL, on age-corrected sNfL percentile levels. **(B)** The same model is shown using a 3-group PRL categorization (0, 1–3, and ≥4 PRL). Platform DMT are glatiramer acetate and interferon beta-1a/b; oral DMT, teriflunomide, dimethyl fumarate, and fingolimod; very-high-efficacy DMT: ocrelizumab, rituximab, natalizumab, mitoxantrone. *Abbreviations:* RRMS, relapsing-remitting MS; PMS, primary/secondary progressive MS, PRL, paramagnetic rim lesions; sNfL, serum neurofilament light chain; EDSS, expanded disability status scale; n.s., non-significant (p≥0.05).

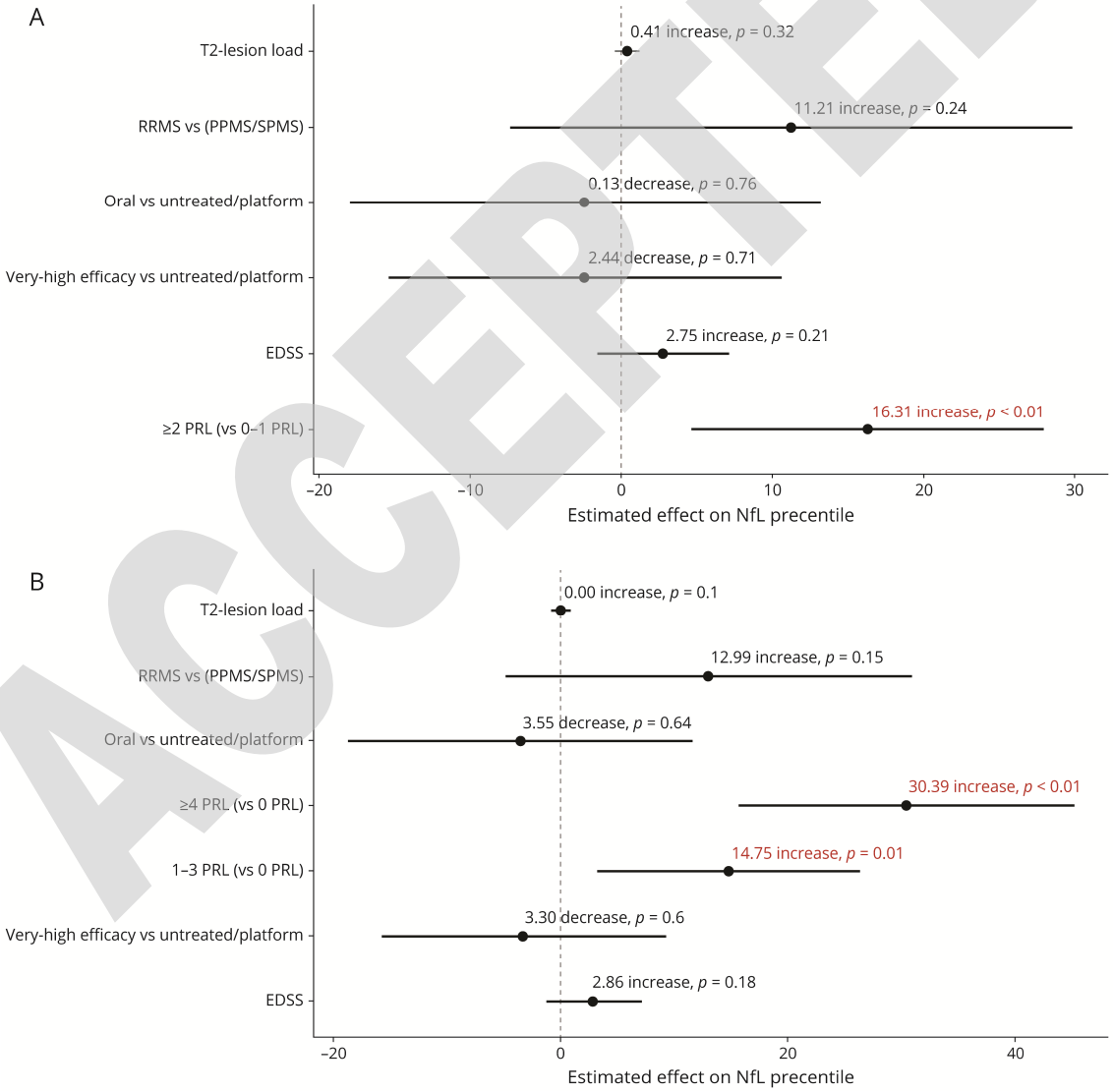

Figure 3. Acute axonal damage in chronic active, smoldering, and chronic inactive lesions. (A) Double immunohistochemistry for MBP (blue) with APP (brown) or CD68 (clone KiM1P) at the lesion edge and center of chronic active, smoldering, and chronic inactive lesions. Insets highlight CD68 positive phagocytes containing MBP positive particles. **(B–D)** Quantification of APP positive (APP+) spheroids at the lesion edge (LE) and center (LC) of chronic active lesions (n=6; Mann-Whitney U test, p=0.004), smoldering lesions (n=9; Mann-Whitney U test, p=0.0002), and chronic inactive lesions (n=6; Mann-Whitney U test, p=0.46). **(E)** Correlation of the density of APP+ spheroids with the density of CD68+ macrophages/activated microglia at the lesion border of chronic active/smoldering and chronic inactive lesions (n=21; r=0.8648; p<0.0001; nonparametric Spearman correlation). *Abbreviations:* MBP, myelin-basic-protein; CD68, CD68-macrophage/activated microglia antibody (clone KiM1P); APP, human-β-amyloid-precursor-protein.

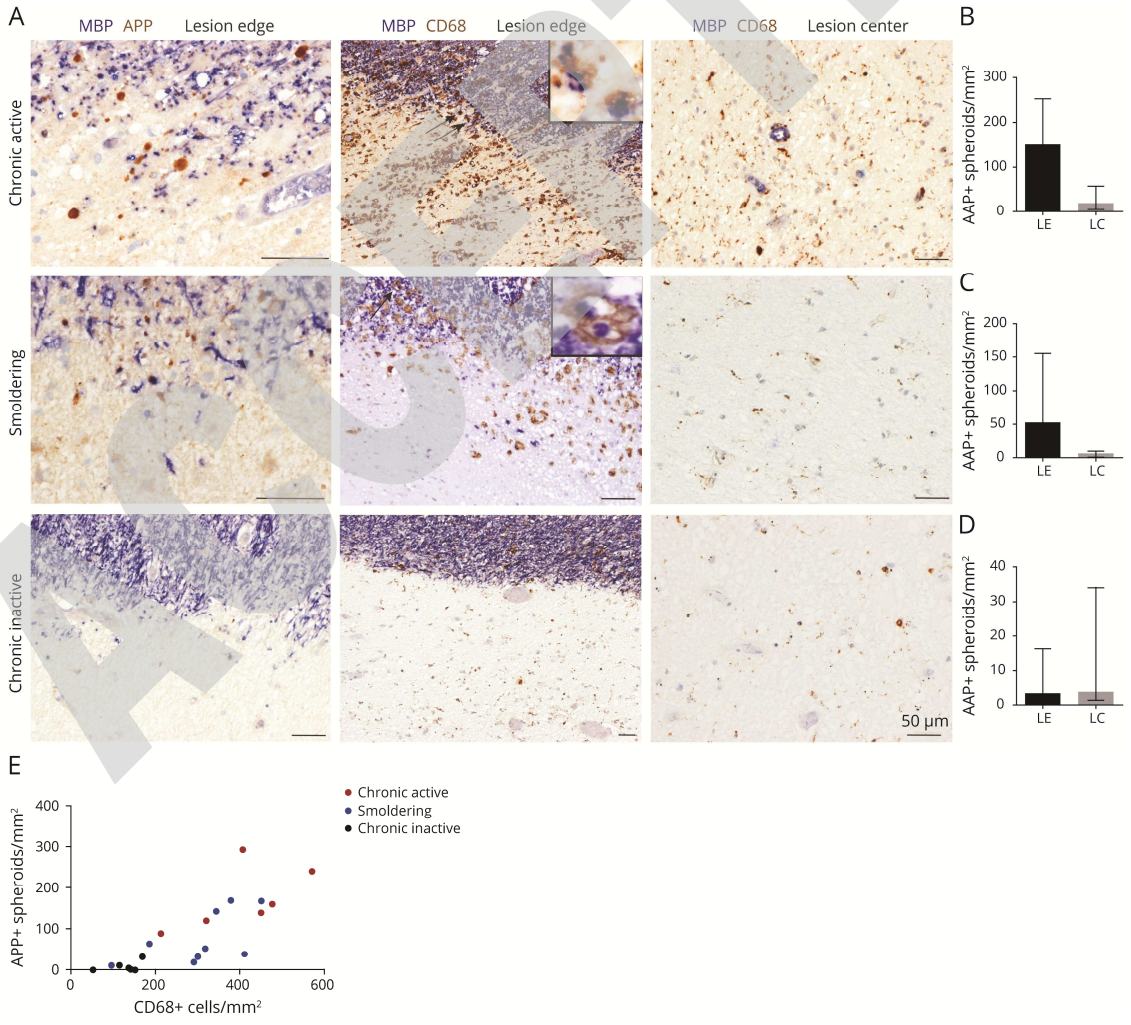

Figure 4. MRI-pathology of paramagnetic rim lesions. Matched MRI-histopathological assessment of one representative chronic active lesion in the cerebral white matter of a 59-year-old PMS case (disease duration 24 years, EDSS=8). The paramagnetic rim visible on the postmortem 3D-EPI phase (red arrows) corresponds on histopathology to an actively inflammatory demyelinating edge of MHC II+ macrophages/microglia containing MBP+ myelin degradation products (MBP-MHC II) and iron (Turnbull-iron). APP+ acutely injured axons are found at the demyelinated lesion edge (MBP-APP). *Abbreviations:* MBP, myelin-basic-protein; MHC II, MHC class II clone CR3/43; Turnbull-Iron, 3,3' diaminobenzidine-tetrahydrochloride enhanced Turnbull staining.

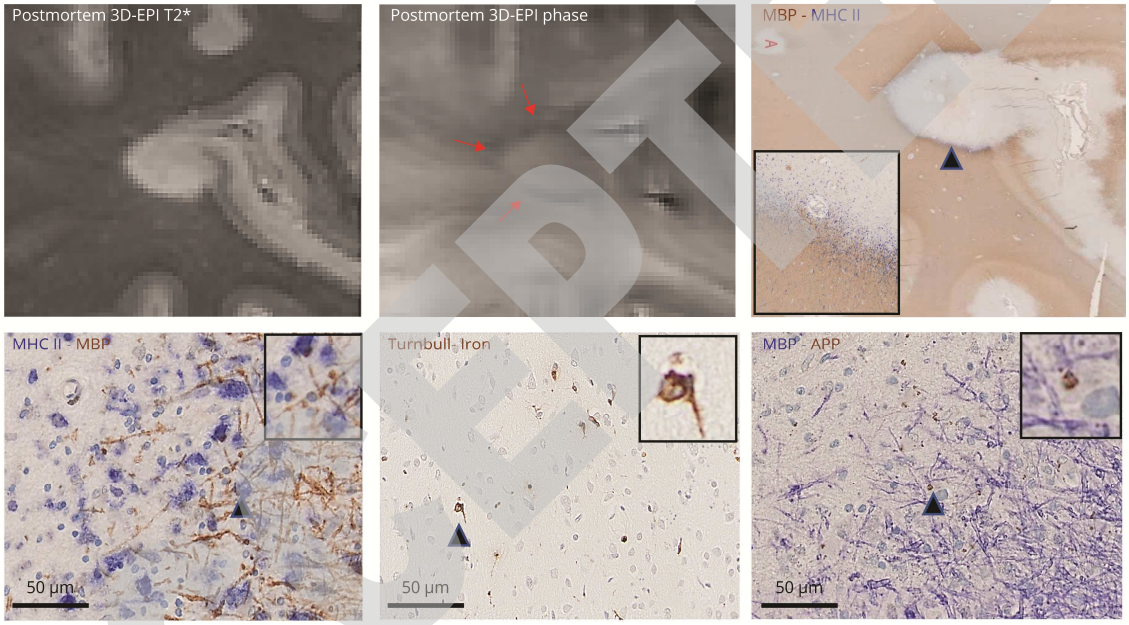

Chronic White Matter Inflammation and Serum Neurofilament Levels in Multiple Sclerosis

Pietro Maggi, Jens Kuhle, Sabine Schädelin, et al.

Neurology published online June 4, 2021
DOI 10.1212/WNL.0000000000012326